Cancer Prevention Research

Research Article
See Perspective on p. 1337

Metabolic Profiling, a Noninvasive Approach for the Detection of Experimental Colorectal Neoplasia

David C. Montrose[1], Xi Kathy Zhou[2], Levy Kopelovich[4], Rhonda K. Yantiss[3], Edward D. Karoly[5], Kotha Subbaramaiah[1], and Andrew J. Dannenberg[1]

Abstract

Colorectal cancer is the second leading cause of cancer-related deaths in the United States. Although noninvasive stool-based screening tests are used for the early detection of colorectal neoplasia, concerns have been raised about their sensitivity and specificity. A metabolomics-based approach provides a potential noninvasive strategy to identify biomarkers of colorectal carcinogenesis including premalignant adenomas. Our primary objective was to determine whether a distinct metabolic profile could be found in both feces and plasma during experimental colorectal carcinogenesis. Feces, plasma as well as tumor tissue and normal colorectal mucosa were obtained from A/J mice at several time points following administration of azoxymethane or saline. Ultra-performance liquid chromatography tandem mass spectroscopy and gas chromatography mass spectroscopy were used to quantify metabolites in each of these matrices. Here, we show that colorectal carcinogenesis was associated with significant metabolic alterations in both the feces and plasma, some of which overlap with metabolic changes in the tumor tissue. These consisted of 33 shared changes between feces and tumor, 14 shared changes between plasma and tumor, and 3 shared changes across all 3 matrices. For example, elevated levels of sarcosine were found in both tumor and feces whereas increased levels of 2-hydroxyglutarate were found in both tumor and plasma. Collectively, these results provide evidence that metabolomics can be used to detect changes in feces and plasma during azoxymethane-induced colorectal carcinogenesis and thus provide a strong rationale for future studies in humans. *Cancer Prev Res; 5(12); 1358–67. ©2012 AACR.*

Introduction

Colorectal cancer (CRC) is the second leading cause of cancer-related deaths in the United States (1). In most cases, CRC evolves over a number of years (2, 3), providing a window of opportunity for early detection and potential intervention to increase survival. To maximize the public health benefit, the optimal screening test should be noninvasive, widely available, and affordable. A test should be able to detect both advanced precursor lesions and curable cancers throughout the colorectum. Although noninvasive fecal blood tests have been widely used, these tests have limited sensitivity for CRC and even lower sensitivity for advanced adenomas (4–6). Stool DNA (sDNA) testing represents another noninvasive method for detecting neoplasia-derived biomarkers. sDNA testing has been used to identify molecular changes associated with colorectal carcinogenesis including mutated genes and altered methylation patterns (7–10). Recently, large adenomas and early stage CRC were detected using next-generation sDNA testing (8). However, large-scale population studies utilizing sDNA testing are needed to further evaluate the sensitivity and specificity of this approach, particularly at the early stages of CRC. Given the limitations of existing methods, complementary approaches to enhance noninvasive screening of colorectal neoplasia should be explored.

Metabolomics can be used to identify and quantify small molecules in a variety of biologic matrices (11, 12). Data generated by this method enable the identification of potential biomarkers of disease as well as dissection of molecular pathways in pathophysiological conditions including cancer (13–20). However, little is known about the potential use of targeted metabolomics for the identification of biomarkers of intestinal neoplasia in feces or plasma. Here, our main goal was to determine whether metabolic changes can be detected in feces and plasma during azoxymethane (AOM)-induced colorectal carcinogenesis. A second objective was to investigate whether the tumor was a potential source for altered levels of metabolites in feces or plasma. Analyses in the current study detected a large number of altered metabolites in feces and plasma of tumor-bearing mice, including a subset

Authors' Affiliations: Departments of [1]Medicine, [2]Public Health, [3]Pathology and Laboratory Medicine, Weill Cornell Medical College, New York; [4]Division of Cancer Prevention, National Cancer Institute, Bethesda, Maryland; and [5]Metabolon, Inc., Durham, North Carolina

Note: Supplementary data for this article are available at Cancer Prevention Research Online (http://cancerprevres.aacrjournals.org/).

Corresponding Author: Andrew J. Dannenberg, Department of Medicine and Weill Cornell Cancer Center, 525 East 68th St., Room F-206, New York, NY 10065. Phone: 212-746-4403; Fax: 212-746-4885; Email: ajdannen@med.cornell.edu

doi: 10.1158/1940-6207.CAPR-12-0160

corresponding to increasing tumor burden. In addition, specific metabolic changes overlapped across all 3 sample types. We also found alterations in a number of metabolic pathways in tumor tissue. Our results provide the first evidence that metabolomics can be used to detect changes in feces and plasma that reflect experimental colorectal neoplasia. These findings provide a strong rationale for carrying out human studies with the goal of both defining the metabolic changes that occur in tumor tissue during colorectal carcinogenesis and possibly identifying metabolites in feces or plasma that reflect colorectal neoplasia.

Materials and Methods

AOM administration and sample collection

A/J mice were purchased from The Jackson Laboratory and administered 6 weekly intraperitoneal injections of either AOM (10 mg/kg; Sigma Aldrich; $n = 40$) or 0.9% saline ($n = 35$) beginning at 5 weeks of age (ref. 21; Fig. 1). Mice were maintained on AIN-93G purified diet (Research Diets) during the entire experiment. Feces were collected 3, 5, and 7 weeks after the last injection by placing mice from the AOM and saline-administered groups in empty cages. Following defecation, fecal pellets (average wet fecal weight, 129 mg/cage) were snap frozen. Blood was collected at sacrifice by cardiac puncture for the preparation of plasma 5 and 7 weeks after the last injection. Seven weeks after the last injection, colorectal tumor tissue, and normal colorectal mucosal samples were collected and snap frozen from AOM and vehicle-treated mice, respectively. Feces, plasma, and colorectal tissue were stored at −80°C until shipped to Metabolon, Inc. for analysis. All experiments were approved by the Weill Cornell Medical College Institutional Animal Care and Use Committee.

Assessment of tumor burden

Whole colons were harvested from a separate set of AOM-injected mice 3, 5, and 7 weeks following the last injection and formalin fixed to assess tumor burden. Tumor number and volume were determined in whole mounts following methylene blue staining. Subsequently, colons were Swiss-rolled, paraffin embedded, and subjected to histologic analysis by a gastrointestinal pathologist (R.K. Yantiss) following H&E staining.

Metabolomic analysis

All samples were shipped on dry ice to Metabolon, Inc. for quantification of metabolites. Each sample was accessioned into the Metabolon Laboratory Information Management System (LIMS) and was assigned by the LIMS a unique identifier that was associated with the original source identifier only. This identifier was used to track all sample handling, tasks, results, etc. The samples (and all derived aliquots) were tracked by the LIMS system. All portions of any sample were automatically assigned their own unique identifiers by the LIMS when a new task was created; the relationship of these samples was also tracked.

For sample preparation, water was added to a volume of 5 μL/mg of tissue ($n = 6$/group) and subjected to homogenization by rapid shaking with a stainless steel ball in a Genogrinder 2000 (Glen Mill Inc.). Fecal pellets were first lyophilized then resuspended in water (20 μL/mg of dried sample) before homogenization by rapid shaking as described above. Following homogenization, 100 μL of the tissue or fecal suspensions were used for extraction. One hundred microliters of each plasma sample were directly used for extraction. Samples were prepared using the automated MicroLab STAR system (Hamilton Company). A recovery standard was added before the first step in the extraction process for quality control (QC) purposes. Sample extraction was conducted using an aqueous methanol extraction process to remove the protein fraction while allowing maximum recovery of small molecules. The resulting extract was divided into 4 fractions: 1 for analysis by ultraperformance liquid chromatography tandem mass spectroscopy (UPLC/MS/MS^2; positive mode), 1 for UPLC/MS/MS^2 (negative mode), 1 for gas chromatography mass spectroscopy (GC/MS), and 1 for backup. Samples were placed briefly on a TurboVap (Zymark) to remove the

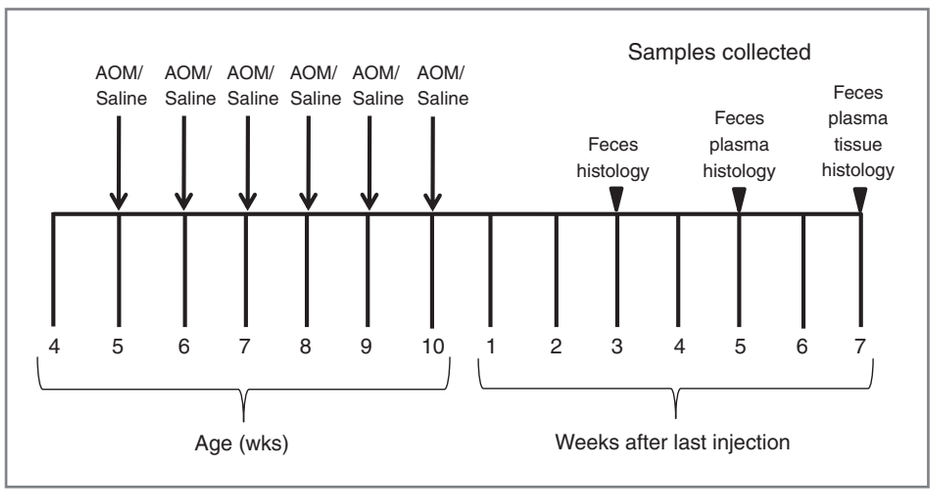

Figure 1. Experimental design Male A/J mice were given 6 weekly intraperitoneal injections of AOM (10 mg/kg; $n = 40$) or 0.9% saline ($n = 35$) beginning at 5 weeks of age. Feces were collected 3, 5, and 7 weeks after the last injection; plasma was collected 5 and 7 weeks after the last injection; tumor tissue from AOM-injected mice and colorectal mucosa from saline-injected mice were harvested 7 weeks after the last injection. Separate groups of mice ($n = 5$ mice/time point) were used to determine tumor burden and histology 3, 5, and 7 weeks following the last AOM injection.

organic solvent. Each sample was then frozen and dried under vacuum and prepared to run on either the UPLC/MS/MS^2 or GC/MS instruments.

Samples were processed as described previously (22, 23). Briefly, the LC/MS portion of the platform was based on a Waters ACQUITY UPLC and a Thermo–Finnigan linear trap quadrupole mass spectrometer, which consists of an electrospray ionization source and linear ion-trap mass analyzer. The sample extract was dried then reconstituted in acidic or basic LC-compatible solvents, each of which contained 8 or more injection standards at fixed concentrations to ensure injection and chromatographic consistency. One aliquot was analyzed using acidic positive ion optimized conditions and the other using basic negative ion optimized conditions in 2 independent injections using separate dedicated columns. Extracts reconstituted in acidic conditions were gradient eluted using water and methanol containing 0.1% formic acid, whereas the basic extracts, which also used water/methanol, contained 6.5 mmol/L ammonium bicarbonate. The MS instrument scanned 99 to 1,000 *m/z* and alternated between MS and data-dependent MS^2 scans using dynamic exclusion with approximately 6 scans per second. Raw data files were archived and extracted as described below. The samples destined for GC/MS analysis were redried under vacuum desiccation for a minimum of 24 hours before being derivatized under dried nitrogen using bis(trimethylsilyl) trifluoroacetamide. The GC column was 5% phenyl and the temperature ramp was from 40° to 300° C in a 16-minute period. Samples were analyzed on a Thermo–Finnigan Trace DSQ fast-scanning single-quadrupole mass spectrometer using electron impact ionization. The information output from the raw data files was automatically extracted as discussed below.

For quality assurance (QA)/QC, additional samples were included with each day's analysis. These samples included extracts of a pool of well-characterized human plasma, extracts of a pool created from a small aliquot of the experimental samples, and process blanks. QC samples were spaced evenly among the injections and all experimental samples were randomly distributed throughout the run. A selection of QC compounds was added to every sample for chromatographic alignment, including those under test.

Instrument variability was determined by calculating the median relative standard deviation (RSD) for the internal standards that were added to each sample before injection into the mass spectrometers. Also included were several technical replicate samples created from a homogeneous pool containing a small amount of all study samples ("Study Matrix"). Overall process variability was determined by calculating the median RSD for all endogenous metabolites (i.e., non-instrument standards) present in 100% of the study matrix samples which are technical replicates of pooled study samples. Values for instrument and process variability in association with these samples met Metabolon's acceptance criteria. Specifically, instrument variability for the internal standards was found to have median RSDs of 4, 5, and 4% for the feces, plasma, and colorectal tissue, respectively. Total process variability for the endogenous biochemicals had median RSDs of 14, 14, and 11% for the feces, plasma and colorectal tissue, respectively.

Raw data were extracted, peak-identified and QC processed using Metabolon's hardware and software. These systems are built on a web-service platform utilizing Microsoft's .NET technologies, which run on high-performance application servers and fiber-channel storage arrays in clusters to provide active failover and load balancing. Metabolon maintains a library based on authenticated standards that contain the retention time/index (RI), mass to charge ratio (*m/z*), and chromatographic data (including MS/MS spectral data) on all molecules present in the library. Furthermore, biochemical identifications are based on 3 criteria: retention index within a narrow RI window of the proposed identification, nominal mass match to the library $+/-$ 0.2 amu, and the MS/MS forward and reverse scores between the experimental data and authentic standards. The MS/MS scores are based on a comparison of the ions present in the experimental spectrum to the ions present in the library spectrum. While there may be similarities between these molecules based on one of these factors, the use of all 3 data points can be used to distinguish and differentiate biochemicals. More than 2,400 commercially available purified standard compounds have been acquired and registered into LIMS for distribution to both the LC and GC platforms for determination of their analytical characteristics. Representative EI fragmentation mass spectra of experimental samples and standards for key metabolites identified in this study are shown in Supplementary Fig. S1.

Quantitative real-time PCR

Total RNA was isolated from frozen tumor tissue or normal colorectal mucosa using the RNeasy mini kit (Qiagen). RNA was reverse transcribed to make cDNA using murine leukemia virus reverse transcriptase and oligo $(dT)_{16}$ primer. The resulting cDNA was used for amplification using QuantiTect Primer Assays (Qiagen) for the following genes: *Phosphoglycerate dehydrogenase* (*PHGDH*; Mm_Phgdh_2_SG); *phosphoserine aminotransferase* (*PSAT1*; Mm_Psat1_2_SG); *phosphoserine phosphatase* (*PSPH*; Mm_Psph_1_SG); *dimethylglycine dehydrogenase* (*DMGDH*; Mm_Dmgdh_1_SG); *sarcosine dehydrogenase* (*SARDH*; Mm_Sardh_1_SG). *Glycine-N-methyltransferase* (*GNMT*) was amplified using the following primer sequences: forward 5′-GGTTGACGCTGGACAAAGAT-3′ and reverse 5′-CAGTCTGGCAAGTGAGCAAA-3′. *Glyceraldehyde 3 phosphate dehydrogenase* was used as an endogenous normalization control for both commercial (Mm_Gapdh_3_SG) and designed primers (forward 5′-AATGTGTCCGTCGTGGATCT-3′ and reverse 5′-CATCGAAGGTGGAAGAGTGG-3′). The amplification products of non-commercial primers were verified by sequencing. Quantitative real-time PCR was conducted using 2× SYBR green PCR master mix on a 7500 real-time PCR system (Applied Biosystems). Relative fold induction was determined using the ddC_T (relative quantification) analysis protocol.

Statistical analysis

Tumor burden in mice at the 3 time points was quantified in terms of tumor number, volume, and the number of invasive lesions. For each of the outcomes, the nonparametric Kruskal–Wallis test was used to compare the difference across the 3 time points. Wilcoxon rank–sum test was then used to compare the outcome measured at any 2 time points of interest. $P < 0.05$ were considered statistically significant.

Metabolomic analyses were carried out for colorectal tissue, feces, and plasma samples. Biochemicals that were detected in at least 1 sample from each group were analyzed. Missing values for the detected biochemicals were imputed with the lowest detected value across all groups. Following log transformation, a flexible Bayesian model-averaging approach was used to examine the effects of AOM treatment, time from treatment and AOM treatment by time interaction on the level of biochemicals measured in different samples (24). False discovery rate (FDR) derived from the posterior inclusion probability of AOM treatment and/or AOM treatment by time interaction effects for each biochemical in a particular sample matrix was obtained. We also calculated the median based fold change and the effect size (25) of differences (i.e., standardized difference) in biochemical levels in samples obtained at each time point comparing the AOM and saline-injected mice. The effect size is defined as $\frac{\bar{x}_{AOM} - \bar{x}_{ctrl}}{s}$, where $\bar{x}_{AOM}$ and $\bar{x}_{ctrl}$ are average metabolite levels in the AOM and the saline-injected groups respectively, s is the pooled standard deviation defined as $\sqrt{\frac{(n_{AOM}-1)s_{AOM}+(n_{ctrl}-1)s_{ctrl}}{n_{AOM}+n_{ctrl}-2}}$ where s_{AOM} and s_{ctrl} are unbiased estimates of standard deviations of the respective study groups and n_{AOM} and n_{ctrl} are the sample sizes of the respective groups (26). Significantly altered biochemicals at all time points were identified by using the following criteria (Criteria 1): (i) FDR< 0.05; (ii) |effect size| > 1 at all time points; and (iii) median based fold-change less than 0.667 or more than 1.5 at all time points. To identify those biochemicals that showed significant time-dependent changes in fecal and plasma samples in association with tumorigenesis, we used the following criteria (Criteria 2): (ii) FDR < 0.05; (ii) effect sizes of AOM versus saline differences at the 3 time points, which either increased or decreased over time; (iii) the difference between effect size at the earliest time point (3 weeks for fecal samples; 5 weeks for plasma samples) and effect size at 7 weeks is greater than 0.8 for every 2 weeks of time difference; (iv) the difference in biochemical levels in terms of effect size and fold-change comparing the AOM and saline groups at 7 weeks reached significance as specified in Criteria 1. The overlap in metabolic changes across the 3 matrices is shown using the Venn diagrams in Fig. 6.

Pathway analysis

Those metabolites significantly changed in tumor tissue as compared with normal mucosa were subjected to Ingenuity Pathway Analysis (IPA) software (Winter release 2011; Ingenuity Systems) to determine molecular interactions (27). KEGG identifiers or Chemical Abstract Service registry numbers and fold changes were uploaded to IPA and each identifier was mapped to its corresponding metabolite in the IPA Knowledgebase. Interactions were then queried between these metabolites and all other metabolites stored within IPA to generate a set of direct interaction networks that were merged. Significantly altered pathways were determined based on the number of molecules altered within a given pathway as determined by the software.

Results

Administration of AOM leads to increased colorectal tumor burden

We first determined colorectal tumor burden in A/J mice 3, 5, and 7 weeks following AOM injections. There was 100% tumor incidence in these mice and methylene blue staining of whole colorectal mounts showed a progressive increase in tumor number (Fig. 2A) and volume (Fig. 2B) over time. Histologic analysis of these tissues revealed mostly noninvasive adenomas at the 3-week time point with a progressive increase in the number of dysplastic lesions with mucosal invasion at 5 and 7 weeks (Fig. 2C).

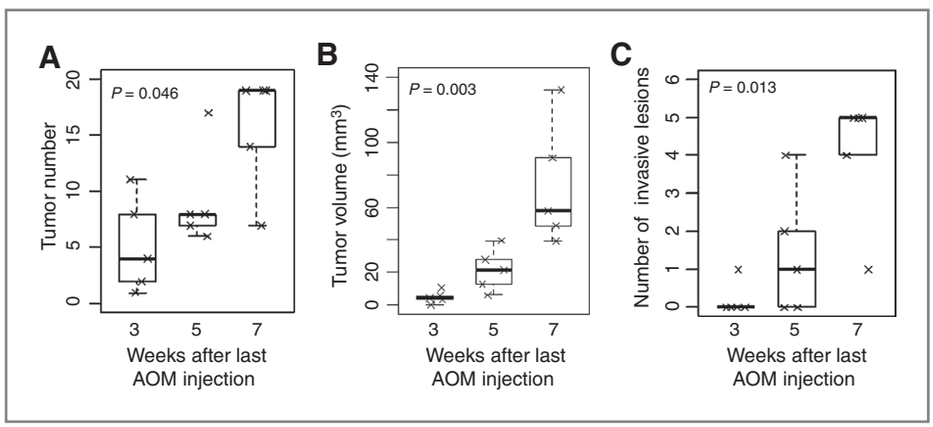

Figure 2. Tumor burden increases over time following AOM administration. A/J mice were administered 6 weekly injections of AOM and sacrificed 3, 5, and 7 weeks after the last injection ($n = 5$/time point). Colorectal tissue was formalin fixed and tumor number (A) and volume (B) determined by examination of whole mounts following methylene blue staining. C, H&E staining was used to determine the number of invasive lesions. P values were determined by the nonparametric Kruskal–Wallis test.

Altered metabolites found in the feces of tumor-bearing mice

To evaluate whether colon carcinogenesis is associated with an altered fecal metabolic profile, feces from AOM versus saline-administered mice were subjected to metabolomic analysis. Significant changes in the levels of 97 metabolites (58 increased and 39 decreased) were found in feces from AOM versus saline-injected mice at 3, 5, and 7 weeks after the last injection (Fig. 3A). These changes included decreased levels of dipeptides and a reciprocal increase in amino acids as well as increased levels of gamma-glutamyl amino acids (Fig. 3A). Interestingly, levels of sarcosine, a metabolite previously implicated in cancer progression (20) increased in the feces of tumor-bearing mice (Fig. 3A). We next investigated whether any metabolic changes in feces correlated with increasing tumor burden. A total of 43 fecal metabolites followed this pattern including 19 that increased and 24 that decreased (Fig. 3B). For example, the levels of heme, a known biomarker of gastrointestinal bleeding, increased during tumor progression.

Colon carcinogenesis is associated with altered metabolites in plasma

The metabolic profile of plasma was next examined from AOM versus saline-treated mice at 5 and 7 weeks after the last injection. A total of 54 metabolites significantly changed at both time points (21 increased and 33 decreased), including a number of bile acids and lipids (Fig. 4A). Notably, levels of 2-hydroxyglutarate (2-HG), a metabolite previously implicated in cancer (28–30), were increased in

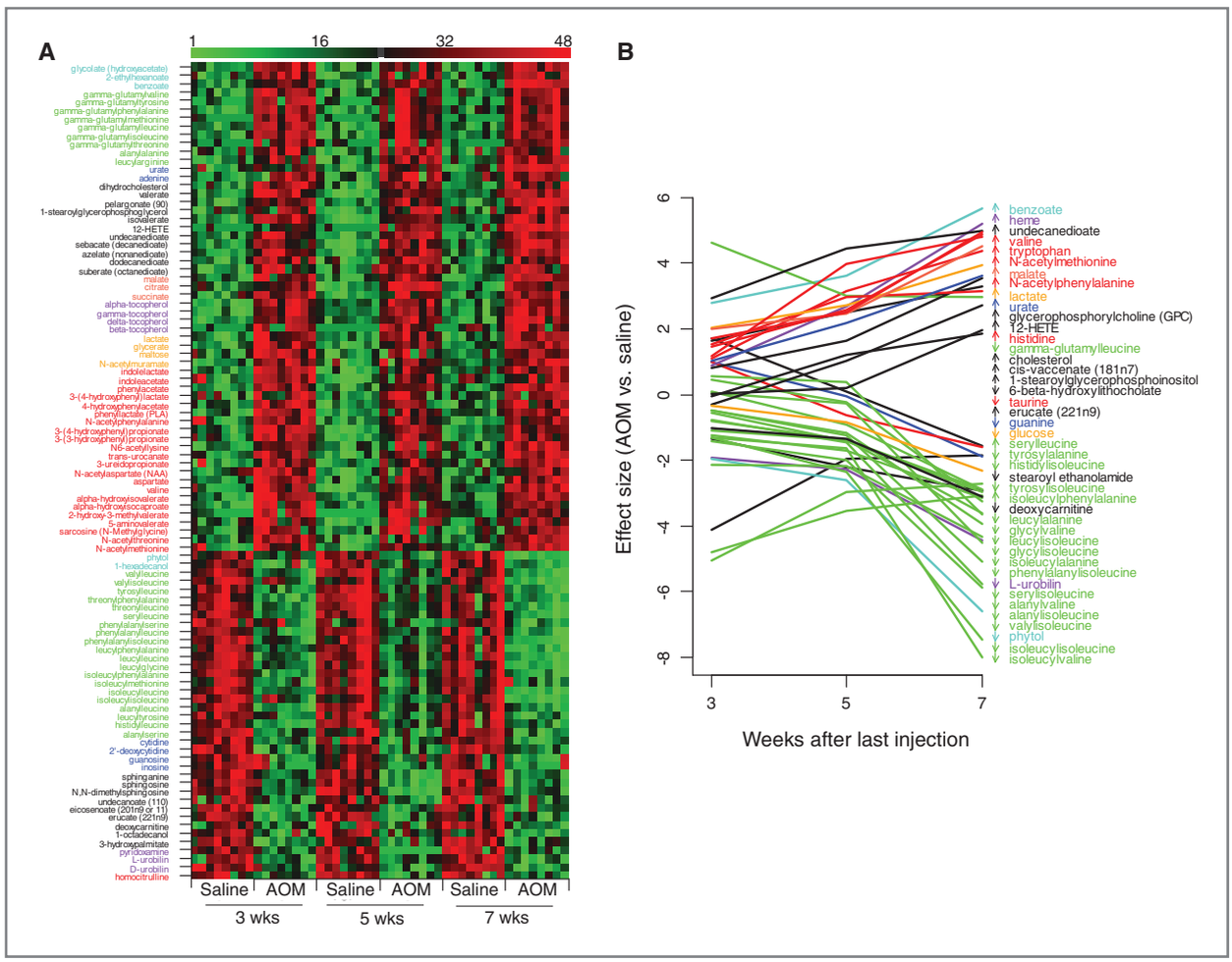

Figure 3. Metabolite levels are altered in feces from colorectal tumor-bearing mice. A/J mice were given 6 weekly injections of either AOM or saline, and feces were collected 3, 5, and 7 weeks following the last injection. Metabolite levels were measured in feces from the saline and AOM-injected mice ($n = 8$/group). A, a heat map of significantly altered metabolites was generated by comparing feces from AOM versus saline injected mice for each time point. Data are rank transformed and displayed as color intensity with low levels indicated by green color and high levels indicated by red color. B, effect size of differences in metabolite levels between mice in AOM and saline-injected groups at different time points following treatment showing time-dependent changes. The effect size is defined as $\frac{\bar{x}_{AOM} - \bar{x}_{ctrl}}{s}$, where $\bar{x}_{AOM}$ and $\bar{x}_{ctrl}$ are the average metabolite levels in the AOM and the saline-injected groups, respectively and s is the pooled standard deviation of metabolite levels measured in the 2 groups. Metabolite names are ordered with respect to the effect size of difference in metabolite levels at 7 weeks. Metabolites in different pathways are color coded in A and B: red font, amino acid; yellow font, carbohydrate; purple font, cofactors and vitamins; orange font, energy; black font, lipids; dark blue font, nucleotides; green font, peptides; and light blue font, xenobiotics.

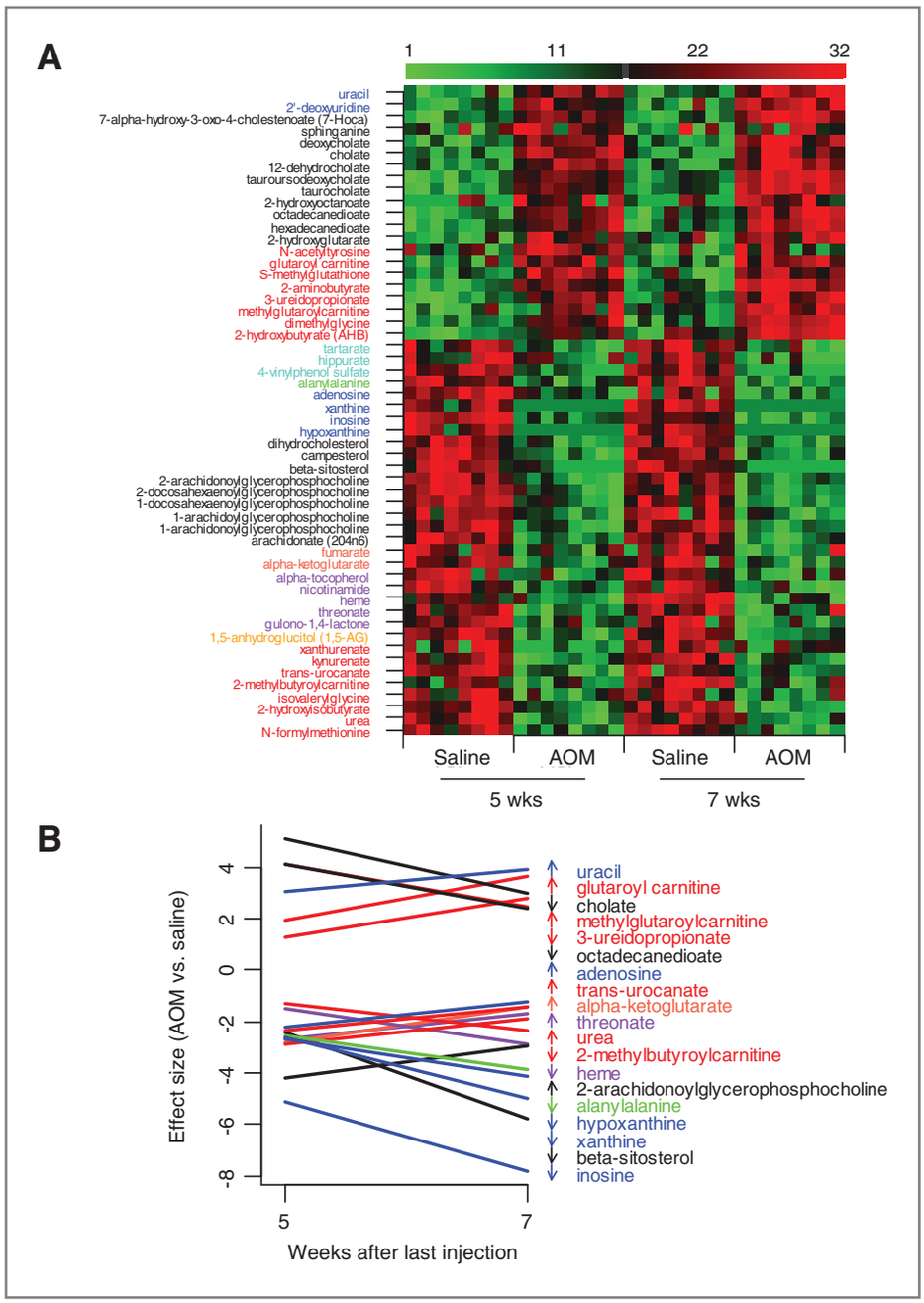

Figure 4. Metabolite levels are altered in plasma from colorectal tumor-bearing mice. A/J mice were given 6 weekly injections of either AOM or saline and plasma was collected 5 and 7 weeks following the last injection. Metabolite levels were measured in plasma from the saline and AOM-injected mice ($n = 8$/group) at each of the 2 time points. A, a heat map of significantly altered metabolites was generated by comparing plasma from AOM versus saline injected mice for each time point. Data are rank transformed and displayed as color intensity with low levels indicated by green color and high levels indicated by red color. B, effect size of differences in metabolite levels between mice in AOM and saline-injected groups at different time points following treatment showing time-dependent change. Metabolite names are ordered with respect to the effect size of difference in metabolite levels at 7 weeks. Metabolites in different pathways are color coded in A and B: red font, amino acid; yellow font, carbohydrate; purple font, cofactors and vitamins; orange font, energy; black font, lipids; dark blue font, nucleotides; green font, peptides; light blue font, xenobiotics.

the plasma of tumor-bearing mice (Fig. 4A). We also examined whether any metabolic changes in plasma correlated with progression of colon carcinogenesis. Nineteen metabolites changed over time including 9 that increased and 10 that decreased (Fig. 4B).

Altered metabolites found in colorectal tumor tissue

Next, we compared the metabolic profiles of colorectal tumors versus normal colorectal mucosa. The levels of 189 metabolites significantly changed including 61 that increased and 128 that decreased in tumor tissue versus normal colorectal mucosa (Fig. 5A–C). Upon categorization of these changes, the largest number of altered metabolites was lipids (14 increased and 63 decreased) and amino acids (29 increased and 13 decreased; Fig. 5A and B). Similar to the findings in feces, tumor tissue also had decreased levels of dipeptides with a concomitant increase in amino acids (Fig. 5B). Levels of additional biochemicals that were changed in tumor tissue included a number of carbohydrates and nucleotides (Fig. 5C). Finally, increased levels of 2-HG and sarcosine, were also found in tumor tissue (Fig. 5A and B).

To determine whether the metabolomic changes found in tumor tissue were consistent with alterations in a

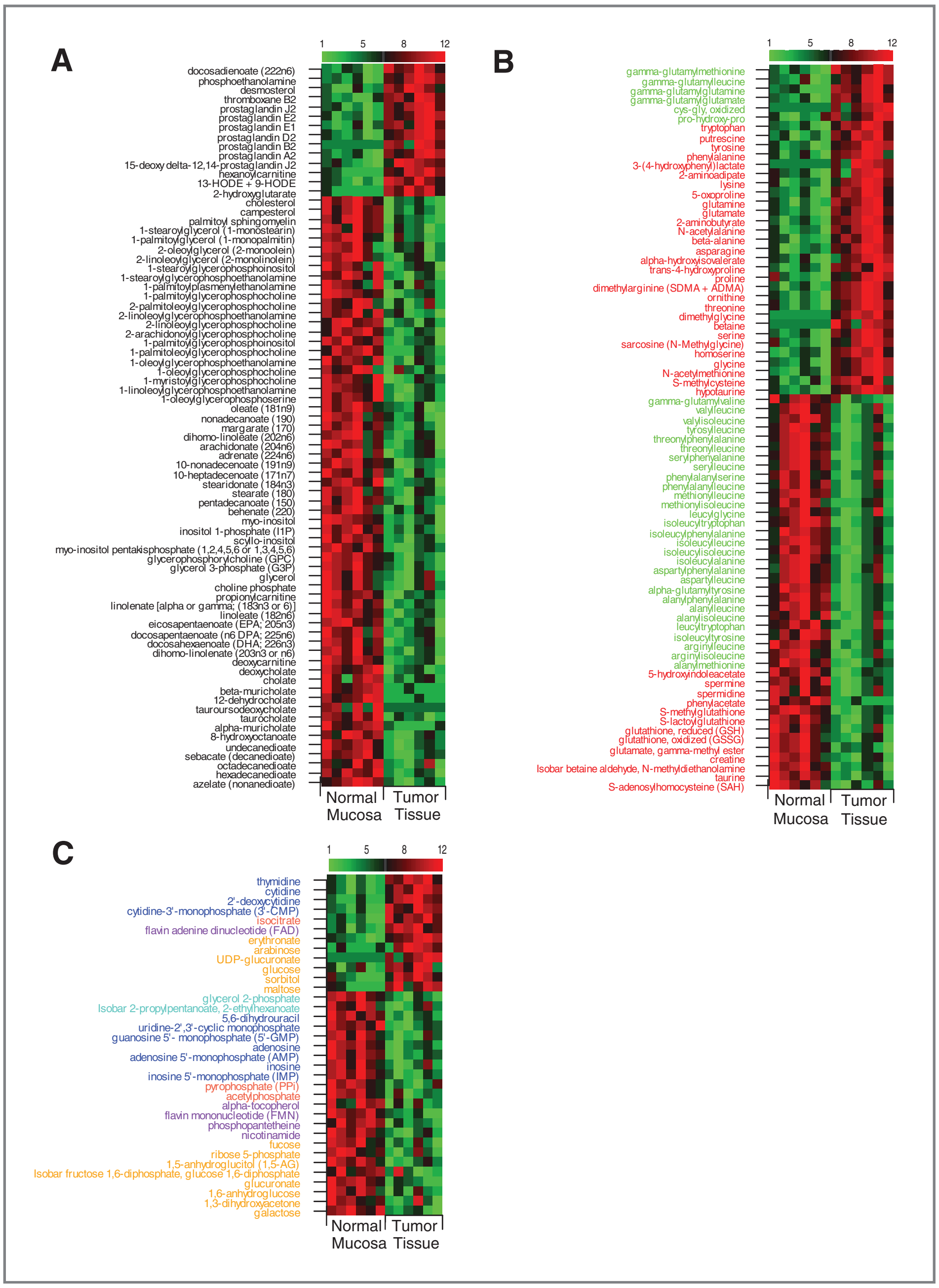

Figure 5. Metabolite levels are altered in colorectal tumor tissue. A/J mice were given 6 weekly injections of either AOM or saline. Seven weeks following the last injection, colorectal mucosa was collected from saline-injected mice and tumor tissue was harvested from AOM-injected mice. Metabolite levels were measured in both tissue types ($n = 6$/group) and significantly altered metabolites were determined by comparing tumor tissue *vs*. normal mucosa. A, lipids. B, amino acids and peptides. C, additional biochemicals. Data are rank transformed and displayed as color intensity with low levels indicated by green color and high levels indicated by red color. Metabolites in different pathways are color coded: red font, amino acid; yellow font, carbohydrate; purple font, cofactors and vitamins; orange font, energy; black font, lipids; dark blue font, nucleotides; green font, peptides; light blue font, xenobiotics.

given metabolic pathway, these data were subjected to IPA. Of the 189 metabolites that were changed in tumor tissue, 97 were identifiable by IPA that showed significant alterations in 22 canonical pathways (Supplementary Fig. S2). Among these pathways, "Glycine, Serine, and Threonine Metabolism" showed increased levels of betaine, dimethylglycine, sarcosine, glycine, and serine (Fig. 5D). Next, we conducted gene expression analysis on the enzymes responsible for the production of these metabolites in tumor tissue and normal colorectal mucosa. As shown in Supplementary Table S1, the levels of enzymes responsible for serine production including PHGDH, PSAT1, and PSPH were all increased in tumor tissue compared with normal mucosa. In addition, the enzymes that generate sarcosine including DMGDH and GNMT were elevated and SARDH that converts sarcosine to glycine, was decreased (Supplementary Table 1).

Metabolic changes that overlap in feces, plasma, and tumor

The results described above indicate that a large number of metabolic changes occur in feces and plasma from tumor-bearing mice as well as in tumor tissue itself. Therefore, we evaluated how many of the significantly changed metabolites were shared by each of the 3 matrices 7 weeks after

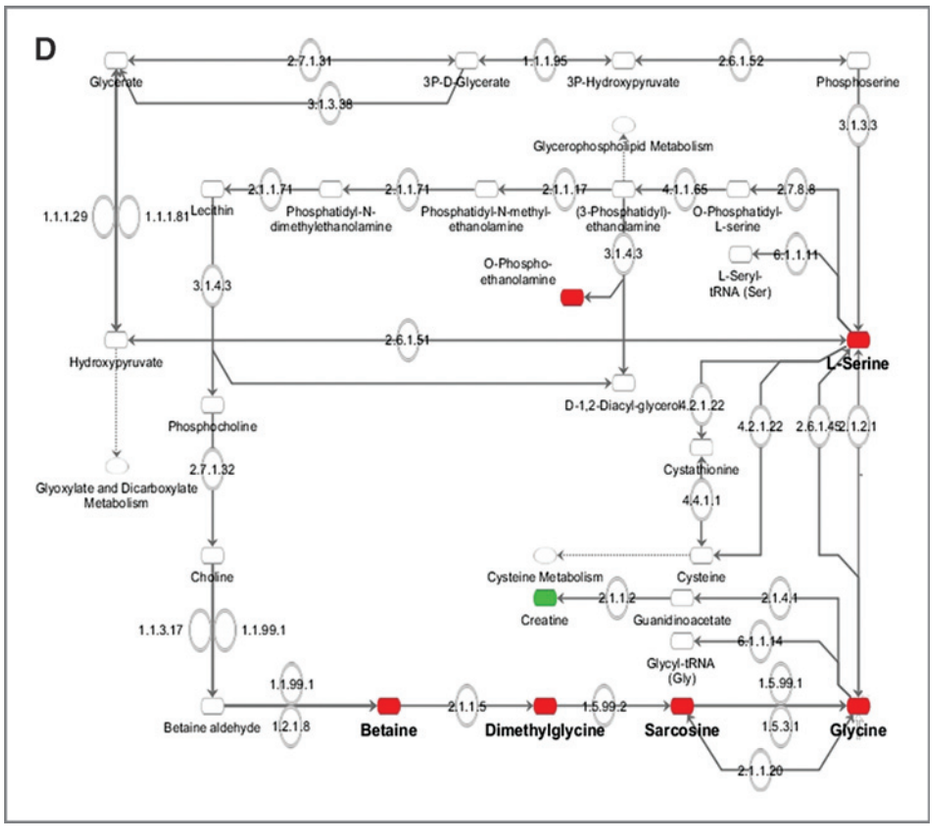

Figure 5. (*Continued*) D, significantly altered metabolites were subjected to IPA and significantly changed metabolites in the "Glycine, Serine, and Threonine Metabolism" canonical pathway are shown. Nodes in red indicate increased levels and nodes in green indicate decreased levels in tumor tissue compared with normal mucosa.

AOM/saline administration. The Venn diagrams in Fig. 6 show 33 shared changes (10 increased, 23 decreased) between feces and tumor, 14 shared changes (4 increased, 10 decreased) between plasma and tumor and 3 shared changes (2 increased, 1 decreased) across all 3 matrices. As expected from our independent analyses of feces and tumor tissue, the shared biochemical changes included mainly amino acids, dipeptides, and lipids. In comparison, fewer metabolomic changes were shared by plasma and tumor that consisted primarily of altered lipid levels. The identity and magnitude of changes in the overlapping metabolites are shown in Supplementary Table 2.

Discussion

Here we show that metabolomic profiling can be used to noninvasively identify novel biomarkers of AOM-induced colorectal neoplasia in mice. Altered metabolite levels were found in feces and plasma of tumor-bearing mice and in tumor tissue itself. In fact, a number of these metabolic changes overlapped across the 3 matrices.

Because colorectal tumors can shed cells or bleed, feces provide a potentially ideal matrix for identifying biomarkers of intestinal neoplasia. To this point, a large number of altered metabolites were detected in the feces of tumor-bearing mice. Ideally, a biomarker should reflect the burden of disease. We identified 43 fecal metabolites including heme that changed with disease progression (Fig. 3B). The fact that levels of heme increased over time is consistent with enhanced gastrointestinal bleeding as tumor burden increased. In humans, the stool guaiac test detects heme and is used to noninvasively screen for colorectal neoplasia (6). The current preclinical results suggest that a large number of metabolites in addition to heme change during colorectal carcinogenesis. If metabolic changes in addition to elevated heme levels can be detected in the feces of humans during colorectal carcinogenesis, it may be possible to develop improved metabolite-based noninvasive testing.

Plasma offers another potential matrix to identify biomarkers of colorectal carcinogenesis. Importantly, our study found a significant number of altered metabolites in the plasma of tumor-bearing mice, including many that changed in association with increased tumor burden (Fig. 4A and B). A number of human studies have also used MS in an effort to identify blood-based signatures of CRC (15, 16, 18, 19). Consistent with prior reports in humans (15, 18), we found altered levels of urea, hippurate, and 2-hydroxybutyrate in tumor-bearing mice (Fig. 4A). We recognize that our ability to tightly control variables that can affect the metabolome including diet, age, gender and gut microbiota may result in different or additional changes than what has been found in humans (11).

Metabolomic analysis can also provide new insights into the deregulation of molecular pathways in tumors. Of interest, serine (a product of phosphoglycerate dehydrogenase activity), sarcosine (an intermediate in glycine

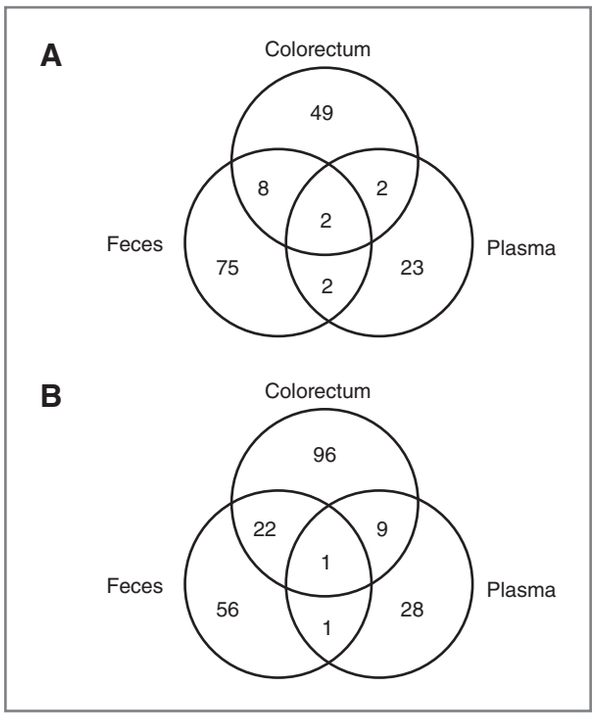

Figure 6. Several metabolite changes are shared across matrices in tumor-bearing versus control mice. The number of significantly altered metabolites was determined in tumor-bearing versus control mice in feces, plasma, and colorectal tissue 7 weeks after the last AOM or saline injection. The number of metabolites whose levels increased (A) or decreased (B) in individual matrices and those that commonly changed across matrices is shown.

metabolism) and 2-HG (a product of glutamate/α-ketoglutarate metabolism) were increased in tumor tissue as compared with normal colorectal mucosa (Fig. 5A and B). The observed expression changes in PHGDH, PSAT, PSPH and DMGDH, SARDH, GNMT within the tumor tissue can explain the increases in serine and sarcosine levels, respectively (Supplementary Table S1). We also note that AOM-induced tumors contain *β-catenin* and K-*ras* mutations that may contribute to these metabolomic changes (31–34).

The relevance of our findings is highlighted by several previous human findings. For example, increased serine levels have been reported in human colon cancer (13, 14). Moreover, a subset of human breast cancers appears to be dependent on the serine synthesis pathway (35). Increased sarcosine levels have been observed in prostate cancer and may play a role in progression (20). The finding of increased 2-HG levels is potentially significant given its association with leukemia and glioma in which mutant isocitrate dehydrogenase contributes to its increased production (28–30). Future studies are warranted to elucidate the functional significance of the observed metabolic changes. Significantly, sarcosine was increased in both feces and tumor tissue, and 2-HG was increased in both plasma and tumor tissue, which may reflect tumor cell shedding. In this regard, changes found in feces and plasma occurred at an early stage of colorectal carcinogenesis (Figs. 3 and 4), highlighting the potential utility of metabolomics for identifying biomarkers of early colorectal lesions. On the basis of the current findings, it will be of considerable interest to determine whether the serine-sarcosine or glutamate-2-HG pathways are altered in human colorectal tumors.

Future studies using this or related metabolomic approaches should be carried out in humans with the goal of both elucidating the metabolic changes that occur in colorectal neoplasia and identifying new biomarkers that have the potential to be useful for the early detection of colorectal neoplasia.

Disclosure of Potential Conflicts of Interest

Edward D. Karoly is an employee of Metabolon, Inc. No potential conflicts of interest were disclosed by the other authors.

Authors' Contributions

Conception and design: D.C. Montrose, L. Kopelovich, E.D. Karoly, K. Subbaramaiah, A.J. Dannenberg,
Development of methodology: D.C. Montrose, L. Kopelovich, A.J. Dannenberg,
Acquisition of data (provided animals, acquired and managed patients, provided facilities, etc.): D.C. Montrose, L. Kopelovich, R.K. Yantiss, A.J. Dannenberg,
Analysis and interpretation of data (e.g., statistical analysis, biostatistics, computational analysis): X.K. Zhou, L. Kopelovich, E.D. Karoly, K. Subbaramaiah,
Writing, review, and/or revision of the manuscript: D.C. Montrose, X.K. Zhou, L. Kopelovich, E.D. Karoly, K. Subbaramaiah, A.J. Dannenberg,
Administrative, technical, or material support (i.e., reporting or organizing data, constructing databases): D.C. Montrose, A.J. Dannenberg,
Study supervision: K. Subbaramaiah, A.J. Dannenberg,

Acknowledgments

The authors would like to express their appreciation to Dr. Steven Gross for numerous helpful discussions.

Grant Support

The project was supported by NCI N01-CN-43302, NIH T32 CA062948, NIH CTSC UL-RR024996, and the New York Crohn's Foundation.

The costs of publication of this article were defrayed in part by the payment of page charges. This article must therefore be hereby marked *advertisement* in accordance with 18 U.S.C. Section 1734 solely to indicate this fact.

Received April 5, 2012; revised July 18, 2012; accepted August 16, 2012; published OnlineFirst September 7, 2012.

References

1. Jemal A, Siegel R, Ward E, Hao Y, Xu J, Thun MJ. Cancer statistics, 2009. CA Cancer J Clin 2009;59:225–49.
2. Beerenwinkel N, Antal T, Dingli D, Traulsen A, Kinzler KW, Velculescu VE, et al. Genetic progression and the waiting time to cancer. PLoS Comput Biol 2007;3:e225.
3. Jones S, Chen WD, Parmigiani G, Diehl F, Beerenwinkel N, Antal T, et al. Comparative lesion sequencing provides insights into tumor evolution. Proc Natl Acad Sci U S A 2008;105:4283–8.
4. Morikawa T, Kato J, Yamaji Y, Wada R, Mitsushima T, Shiratori Y. A comparison of the immunochemical fecal occult blood test and total

colonoscopy in the asymptomatic population. Gastroenterology 2005;129:422–8.
5. Quintero E, Castells A, Bujanda L, Cubiella J, Salas D, Lanas A, et al. Colonoscopy versus fecal immunochemical testing in colorectal-cancer screening. N Engl J Med 2012;366:697–706.
6. van Dam L, Kuipers EJ, van Leerdam ME. Performance improvements of stool-based screening tests. Best Pract Res Clin Gastroenterol 2010;24:479–92.
7. Ahlquist DA. Molecular detection of colorectal neoplasia. Gastroenterology 2010;138:2127–39.
8. Ahlquist DA, Zou H, Domanico M, Mahoney DW, Yab TC, Taylor WR, et al. Next-generation stool DNA test accurately detects colorectal cancer and large adenomas. Gastroenterology 2012;142:248–56; quiz e25–6.
9. Chen WD, Han ZJ, Skoletsky J, Olson J, Sah J, Myeroff L, et al. Detection in fecal DNA of colon cancer-specific methylation of the nonexpressed vimentin gene. J Natl Cancer Inst 2005;97: 1124–32.
10. Zou H, Taylor WR, Harrington JJ, Hussain FT, Cao X, Loprinzi CL, et al. High detection rates of colorectal neoplasia by stool DNA testing with a novel digital melt curve assay. Gastroenterology 2009;136:459–70.
11. Collino S, Martin FP, Rezzi S. Clinical Metabolomics paves the way towards future healthcare strategies. Br J Clin Pharmacol. 2012 [Epub ahead of print].
12. Vinayavekhin N, Homan EA, Saghatelian A. Exploring disease through metabolomics. ACS Chem Biol 2010;5:91–103.
13. Denkert C, Budczies J, Weichert W, Wohlgemuth G, Scholz M, Kind T, et al. Metabolite profiling of human colon carcinoma–deregulation of TCA cycle and amino acid turnover. Mol Cancer 2008;7:72.
14. Hirayama A, Kami K, Sugimoto M, Sugawara M, Toki N, Onozuka H, et al. Quantitative metabolome profiling of colon and stomach cancer microenvironment by capillary electrophoresis time-of-flight mass spectrometry. Cancer Res 2009;69:4918–25.
15. Ikeda A, Nishiumi S, Shinohara M, Yoshie T, Hatano N, Okuno T, et al. Serum metabolomics as a novel diagnostic approach for gastrointestinal cancer. Biomed Chromatogr 2012;26:548–58.
16. Miyagi Y, Higashiyama M, Gochi A, Akaike M, Ishikawa T, Miura T, et al. Plasma free amino acid profiling of five types of cancer patients and its application for early detection. PLoS One 2011;6:e24143.
17. Monleon D, Morales JM, Barrasa A, Lopez JA, Vazquez C, Celda B. Metabolite profiling of fecal water extracts from human colorectal cancer. NMR Biomed 2009;22:342–8.
18. Qiu Y, Cai G, Su M, Chen T, Zheng X, Xu Y, et al. Serum metabolite profiling of human colorectal cancer using GC-TOFMS and UPLC-QTOFMS. J Proteome Res 2009;8:4844–50.
19. Ritchie SA, Ahiahonu PW, Jayasinghe D, Heath D, Liu J, Lu Y, et al. Reduced levels of hydroxylated, polyunsaturated ultra long-chain fatty acids in the serum of colorectal cancer patients: implications for early screening and detection. BMC Med 2010;8:13.
20. Sreekumar A, Poisson LM, Rajendiran TM, Khan AP, Cao Q, Yu J, et al. Metabolomic profiles delineate potential role for sarcosine in prostate cancer progression. Nature 2009;457:910–4.
21. Nakanishi M, Menoret A, Tanaka T, Miyamoto S, Montrose DC, Vella AT, et al. Selective PGE(2) suppression inhibits colon carcinogenesis and modifies local mucosal immunity. Cancer Prev Res (Phila) 2011;4:1198–208.
22. Evans AM, DeHaven CD, Barrett T, Mitchell M, Milgram E. Integrated, nontargeted ultrahigh performance liquid chromatography/electrospray ionization tandem mass spectrometry platform for the identification and relative quantification of the small-molecule complement of biological systems. Anal Chem 2009;81:6656–67.
23. Reitman ZJ, Jin G, Karoly ED, Spasojevic I, Yang J, Kinzler KW, et al. Profiling the effects of isocitrate dehydrogenase 1 and 2 mutations on the cellular metabolome. Proc Natl Acad Sci U S A 2011; 108:3270–5.
24. Zhou XK LF, Dannenberg AJ. A Bayesian model averaging approach for observational gene expression studies. Ann Appl Stat 2012;6: 497–520.
25. Ellis PD. The essential guide to effect sizes: statistical power, meta-analysis, and the interpretation of research results. Cambridge: Cambridge University Press, 2010.
26. Olejnik S, Algina J. Measures of effect size for comparative studies: applications, interpretations, and limitations. Contemp Educ Psychol 2000;25:241–86.
27. Dong H, Zhang A, Sun H, Wang H, Lu X, Wang M, et al. Ingenuity pathways analysis of urine metabolomics phenotypes toxicity of Chuanwu in Wistar rats by UPLC-Q-TOF-HDMS coupled with pattern recognition methods. Mol Biosyst 2012;8:1206–21.
28. Dang L, White DW, Gross S, Bennett BD, Bittinger MA, Driggers EM, et al. Cancer-associated IDH1 mutations produce 2-hydroxyglutarate. Nature 2009;462:739–44.
29. Figueroa ME, Abdel-Wahab O, Lu C, Ward PS, Patel J, Shih A, et al. Leukemic IDH1 and IDH2 mutations result in a hypermethylation phenotype, disrupt TET2 function, and impair hematopoietic differentiation. Cancer Cell 2010;18:553–67.
30. Ward PS, Patel J, Wise DR, Abdel-Wahab O, Bennett BD, Coller HA, et al. The common feature of leukemia-associated IDH1 and IDH2 mutations is a neomorphic enzyme activity converting alpha-ketoglutarate to 2-hydroxyglutarate. Cancer Cell 2010;17: 225–34.
31. Bolt AB, Papanikolaou A, Delker DA, Wang QS, Rosenberg DW. Azoxymethane induces KI-ras activation in the tumor resistant AKR/J mouse colon. Mol Carcinog 2000;27:210–8.
32. Erdman SH, Wu HD, Hixson LJ, Ahnen DJ, Gerner EW. Assessment of mutations in Ki-ras and p53 in colon cancers from azoxymethane- and dimethylhydrazine-treated rats. Mol Carcinog 1997;19:137–44.
33. Takahashi M, Fukuda K, Sugimura T, Wakabayashi K. Beta-catenin is frequently mutated and demonstrates altered cellular location in azoxymethane-induced rat colon tumors. Cancer Res 1998;58:42–6.
34. Takahashi M, Nakatsugi S, Sugimura T, Wakabayashi K. Frequent mutations of the beta-catenin gene in mouse colon tumors induced by azoxymethane. Carcinogenesis 2000;21:1117–20.
35. Possemato R, Marks KM, Shaul YD, Pacold ME, Kim D, Birsoy K, et al. Functional genomics reveal that the serine synthesis pathway is essential in breast cancer. Nature 2011;476:346–50.